Research Article

Intranasal insulin ameliorates neurological impairment after intracerebral hemorrhage in mice

https://doi.org/10.4103/1673-5374.314320

Date of submission: December 9, 2020

Date of decision: February 2, 2021

Date of acceptance: April 2, 2021

Date of web publication: June 7, 2021

Yuan Zhu[1, 2, #], Yi Huang[1, 2, #], Jin Yang[3], Rong Tu[1, 2], Xin Zhang[1, 2], Wei-Wei He[1, 2], Chang-Yue Hou[1, 2], Xiao-Ming Wang[1, 2], Ju-Ming Yu[1, 2, *], Guo-Hui Jiang[1, 2, *]

Graphical Abstract *Neuroprotection of intranasal insulin in intracerebral hemorrhage*

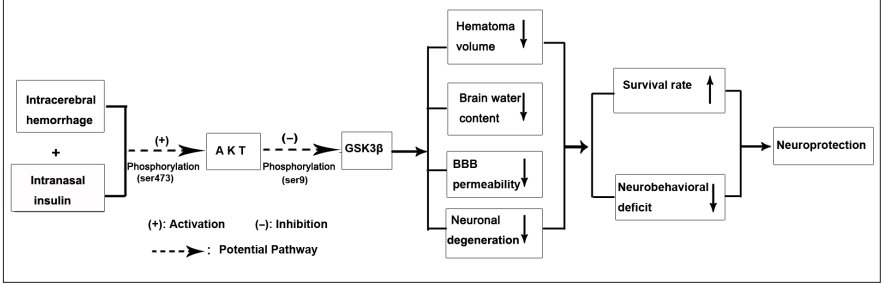

Abstract

In Alzheimer's disease and ischemic stroke, intranasal insulin can act as a neuroprotective agent. However, whether intranasal insulin has a neuroprotective effect in intracerebral hemorrhage and its potential mechanisms remain poorly understood. In this study, a mouse model of autologous blood-induced intracerebral hemorrhage was treated with 0.5, 1, or 2 IU insulin via intranasal delivery, twice per day, until 24 or 72 hours after surgery. Compared with saline treatment, 1 IU intranasal insulin treatment significantly reduced hematoma volume and brain edema after cerebral hemorrhage, decreased blood-brain barrier permeability and neuronal degeneration damage, reduced neurobehavioral deficits, and improved the survival rate of mice. Expression levels of p-AKT and p-GSK3β were significantly increased in the perihematoma tissues after intranasal insulin therapy. Our findings suggest that intranasal insulin therapy can protect the neurological function of mice after intracerebral hemorrhage through the AKT/GSK3β signaling pathway. The study was approved by the Ethics Committee of the North Sichuan Medical College of China (approval No. NSMC(A)2019(01)) on January 7, 2019.

Key Words: AKT; blood-brain barrier; brain edema; glycogen synthase kinase-3; hematoma; insulin; intracerebral hemorrhage; intranasal insulin; neurological impairment; neuronal degeneration; neuroprotection

Chinese Library Classification No. R453; R743.34; R364

Introduction

Intracerebral hemorrhage (ICH) is a subtype of stroke with high incidence, mortality, disability, and recurrence rates, and is the principal cause of death and disability worldwide (Krishnamurthi et al., 2013; GBD 2016 Stroke Collaborators, 2019), particularly in Asia and low- and middle-income countries (An et al., 2017). Despite ongoing research, effective therapies for ICH are still quite limited. Thus, novel treatments and therapeutic targets for ICH should be explored.

ICH induces primary and secondary brain injuries. The primary injury is the destruction of brain structures caused by the space-occupying effect and mechanical compression of hematomas (Zheng et al., 2016). Secondary injury is associated with brain edema, apoptosis, neuronal degeneration and necrosis, inflammatory response, and thrombin formation (Shao et al., 2019). Increased permeability and destruction of the blood-brain barrier (BBB) promotes inflammatory cell infiltration and vasogenic brain edema formation, which exacerbates secondary brain injury (Keep et al., 2018). Current ICH treatments mainly target the primary injury and do not reduce mortality or improve prognosis (Keep et al., 2012).

Peripheral insulin can enter the central nervous system through the BBB and bind to receptors on target cells in the brain to exert a variety of biological effects such as maintaining energy metabolism homeostasis, and regulating neuronal growth and differentiation (Ghasemi et al., 2013; Begg, 2015; Zeng et al., 2016). Insulin resistance in the brain plays an important role in the pathophysiology of a variety of neurological diseases including Alzheimer's disease and stroke (Wieberdink et al., 2012; Arnold et al., 2018). Additionally, insulin resistance is an important risk factor for acute cerebrovascular disease (Kernan et al., 2002) and is closely associated with BBB disruption (Rhea and Banks, 2019). Therefore, increasing brain insulin levels, regulating the insulin

[1]Department of Neurology, Affiliated Hospital of North Sichuan Medical College, Nanchong, Sichuan Province, China; [2]Institute of Neurological Diseases, North Sichuan Medical College, Nanchong, Sichuan Province, China; [3]Department of Intensive Care Unit, Affiliated Hospital of North Sichuan Medical College, Nanchong, Sichuan Province, China

*Correspondence to: Guo-Hui Jiang, MD, neurodoctor@163.com; Ju-Ming Yu, MD, yujuming1963@126.com.
https://orcid.org/0000-0002-1267-2221 (Guo-Hui Jiang); https://orcid.org/0000-0003-1964-4634 (Ju-Ming Yu)
#Both authors contributed equally to this work.

Funding: *This work was supported by the National Natural Science Foundation of China, No. 81971220; and a grant from the Science and Technology Department of Sichuan Province of China, No. 2018JY0236 (both to GHJ).*

How to cite this article: *Zhu Y, Huang Y, Yang J, Tu R, Zhang X, He WW, Hou CY, Wang XM, Yu JM, Jiang GH (2022) Intranasal insulin ameliorates neurological impairment after intracerebral hemorrhage in mice. Neural Regen Res 17(1):210-216.*

signaling pathway, and improving insulin resistance may be potential treatments for neurological diseases.

Intranasal delivery of insulin is safe, non-invasive, and rapidly effective. Intranasal insulin directly accesses the brain through the olfactory and trigeminal nerve pathways, and rapidly increases the insulin concentration in the brain (Santiago and Hallschmid, 2019). Intranasal insulin may alleviate cognitive dysfunction via activation of the phosphoinositide 3-kinase/AKT/glycogen synthase kinase 3β (GSK3β) signaling pathway (Yang et al., 2013; Gabbouj et al., 2019; Lv et al., 2020). Insulin intervention in ischemic stroke accelerates AKT phosphorylation, increases cerebral blood flow and neuronal survival, reduces cell apoptosis, and thus reduces the infarct area and improves functional outcomes (Huang et al., 2014; Lioutas and Novak, 2016). Inhibiting the expression of GSK3β, a signaling molecule downstream of AKT, has been shown to reduce the neurological damage caused by ischemic stroke (Xiao et al., 2017). However, the potential neuroprotective effects of intranasal insulin for ICH remain unclear. ICH has some of the same pathophysiological processes as ischemic stroke. Hence, we hypothesize that intranasal insulin alleviates ICH-induced brain tissue injury through the AKT/GSK3β insulin signaling pathway by activating AKT and inhibiting GSK3β.

In this study, we used the autologous blood-induced hemorrhage mouse model to investigate whether intranasal insulin can improve neurologic injury induced by ICH. We also explored whether its effect was associated with the AKT/GSK3β insulin signaling pathway.

Materials and Methods

Animals

Estrogen has a protective effect on blood vessels and against ICH (Auriat et al., 2005; Ramesh et al., 2019). For homogeneity and to avoid the impact of the estrous cycle on the results, we used only male animals. Clean-grade male C57BL/6J mice (6–8 weeks old, weighing 22–25 g) were purchased from the Laboratory Animal Center of the North Sichuan Medical College (license No. SCXK (Chuan) 2018-18). During the study, the mice were housed in a controlled environment with suitable temperature and humidity, a 12-hour day/night cycle, and free access to water and food. All procedures and animal experiments in this study were performed in accordance with the requirements of the Institutional Animal Care and Use Committee and approved by the Ethics Committee of the North Sichuan Medical College (approval No. NSMC(A)2019(01)) on January 7, 2019. Mice were randomly divided into the following groups (n = 35 per group): (1) sham group, (2) ICH mice treated with intranasal normal saline, (3) ICH mice treated with 0.5 IU intranasal insulin, (4) ICH mice treated with 1 IU intranasal insulin, and (5) ICH mice treated with 2 IU intranasal insulin.

ICH model

The autologous blood-induced hemorrhage model was prepared according to the protocol described in a previous study (Chang et al., 2011). In brief, the randomly selected mice were anesthetized inside a clean induction chamber with 3–4% isoflurane (RWD Life Science, Shenzhen, China) in oxygen (flow rate, 2 L/min). The anesthetized mice were then positioned on a stereoscopic locator (Stoelting, Wood Dale, IL, USA). Intraoperatively, anesthesia was maintained with a face mask with 1–2% isoflurane and an oxygen flow of 1 L/min. Ophthalmic scissors were used to remove the hair from the top of the head. A burr hole was drilled with a 1 mL syringe after the skull seam was exposed (0.8 mm anterior and 2 mm left lateral to bregma (Zhou et al., 2017). A total of 25 μL of tail venous blood, obtained by cutting off approximately 3 mm of the tail tip, was collected with a 100 μL Hamilton microsyringe (Hamilton, Reno, NV, USA) moistened with normal saline in advance, and was then injected into the striatum via the burr hole at a rate of 2 μL/min (3.5 mm depth relative to bregma). The needle was left in place for 10 minutes, and was then pulled out slowly and uniformly. The burr hole was closed with bone wax and the scalp was sutured. An equal volume (25 μL) of saline was injected into the sham control mice. After the operation, the mice had free access to food and water. The success rate of the model was 88%; failed models [neurological deficit score (NDS) < 4] and dead mice during the operation were excluded from the study. Excluded animals were replaced such that each group had an equal number of animals.

Intranasal insulin treatment

Normal saline and insulin (Novo Nordisk, Tianjin, China) were administered into the nose slowly with a 10 μL pipette twice a day from the first day after the surgery until 24 or 72 hours after the surgery.

Survival analysis

The number of dead mice was calculated every hour after ICH. The following equation was used to calculate the survival rate (%): (total number of mice per group – number of deaths per group)/total number of mice per group × 100. Kaplan-Meier survival analysis was then conducted to evaluate survival rates (Meng et al., 2017).

Neurological impairment assessment

Neurological impairment was assessed by using the NDS, a 28-point neurological scoring system (Clark et al., 1998), which contains seven tests: body symmetry, gait, climbing, circling behavior, front limb symmetry, compulsory circling and whisker response (**Additional Table 1**). The surviving mice in each group were scored at 24 and 72 hours after ICH by an investigator who was blind to the experimental treatment groups. A lower score indicates better neurological function.

Brain water content measurement

Mice were selected randomly from each experimental group (n = 6 per group) and sacrificed by decapitation after being anesthetized with an intraperitoneal injection of 1% pentobarbital sodium (Micklin, Shanghai, China) at 24 or 72 hours after the surgery. Their brains were removed immediately and dissected into three parts: two cerebral hemispheres (2 mm anterior and 4 mm posterior to the bregma) and the cerebellum. Each part was placed into an Eppendorf tube that had been marked and weighed in advance, and was then weighed immediately on an analytical balance (Mettler Toledo, Shanghai, China) to determine the wet weight. Afterwards, all of the Eppendorf tubes were heated in an oven at 100°C for 24 hours to acquire the tissue dry weight. The following formula was used to compute the brain water content (%): (wet weight – dry weight)/(wet weight) × 100 (Zhu et al., 2014).

Evaluation of BBB permeability

BBB permeability in mice at 24 and 72 hours after surgery was evaluated through Evans blue staining (Wang et al., 2016). Briefly, Evans blue (Sigma-Aldrich, St. Louis, MO, USA) was diluted with 0.9% saline to a 2% solution. The dye solution was then administered slowly (4 mL/kg) through the caudal veins of the mice. Mice were perfused with ice-cold phosphate-buffered saline after the stain had circulated for 3 hours. The left hemisphere was separated as a sample and stored at –80°C for use. Formamide (2 mL/g of tissue) was added to the samples that were weighed. The mixture was placed in a water bath with a constant temperature of 60°C for 24 hours, and then centrifuged (15 minutes, 10,000 r/min, 4°C) to collect the supernatant. The Evans blue content of the supernatant was measured with a spectrophotometer (Beckman Coulter, Fullerton, CA, USA) at 630 nm and then quantified according to a standard curve. The Evans blue leakage was represented

as micrograms of Evans blue stain per gram of brain tissue weight.

Hematoma measurement

Mice were anesthetized either 24 or 72 hours (n = 3 per group) after the operation with 1% pentobarbital sodium and then perfused with precooled phosphate-buffered saline, followed by continuous perfusion with 4% paraformaldehyde. The brains were removed and fixed with 4% paraformaldehyde immediately after perfusion. The cerebellum was removed and the fixed brains were embedded in optimal cutting temperature compound (SAKURA, Torrance, CA, USA) and serial sliced coronally with a thickness of 100 μm in a cryostat (CM1900, Leica Microsystems, Wetzlar, Germany). Photos were taken of the slices at the same time as they were sectioned. ImageJ software1.6.0-20 (Media Cybernetics, Bethesda, MD, USA) was used to analyze the photographs and to measure the volume of the hematoma. The total hematoma volume was expressed by multiplying the total area of the clot in each section and the distance between the sections (Song et al., 2003).

Evaluation of neuronal degeneration

Neuronal degeneration was evaluated by Fluoro-Jade B (FJB) staining. Mice were perfused with phosphate-buffered saline, followed immediately by 4% paraformaldehyde, and their brains were fixed in paraformaldehyde for 24 hours. The brains were then successively placed into a 15% and then 30% sucrose solution for dehydration, and cryosectioned into coronal sections. Frozen sections were dried at 50°C for 30 minutes and soaked in 80% alcohol containing 1% NaOH for 5 minutes, followed by soaking in 70% alcohol by immersion for 2 minutes. After being washed in distilled water for 2 minutes, the sections were transferred to a 0.06% potassium permanganate solution for 10 minutes at room temperature. The sections were rinsed in distilled water again for 2 minutes, and 0.004% FJB dye solution (Chemicon International, Temecula, CA, USA) was added for staining in the dark at room temperature for 20–40 minutes. The slices were washed in distilled water three times for 1 minute each followed by drying with a hair dryer, and were then immersed in dimethylbenzene for 5 minutes. Neutral balsam was used to seal the slices. Photos of FJB-positive cells in perihematomal tissue (three mice per group and one tissue slice per mouse) were taken using a fluorescence microscope (Olympus, Tokyo, Japan). The excitation wavelength was 488 nm (green) and the emission light was detected with a 520-nm band-pass filter. ImageJ software was used to calculate the number of positive cells, and analyzed with three different units of the perihematomal tissue in each slice, which was regarded as the average number of positive cells in each slice (Liu et al., 2017).

Western blot assay

Mice (n = 6 per group) were euthanized for western blot analysis 24 hours after surgery. Their brains were removed immediately after they were anesthetized by intraperitoneal injection of 1% pentobarbital sodium, and the perihematoma tissue was isolated. The samples were homogenized in radioimmunoprecipitation assay buffer (P0013E, Beyotime Biotechnology, Shanghai, China) containing protease and phosphatase inhibitors, and then centrifuged for 15 minutes at 12,000 r/min and 4°C to collect the supernatant. The protein concentration was measured by Bicinchoninic acid Protein Assay Kit (P0010, Beyotime Biotechnology). Equal amounts (30 μg) of total protein were separated on 10% sodium dodecyl sulfate-polyacrylamide gel electrophoresis gels and transferred to polyvinylidene difluoride membranes (Pall Crop., East Hills, NY, USA). The polyvinylidene difluoride membranes were blocked with 5% skim milk for 2 hours and then incubated at 4°C with primary antibodies overnight. The following primary antibodies were used in this experiment: rabbit anti-AKT polyclonal antibody (1:500, Cat# 40567, Signalway Antibody [SAB], College Park, MD, USA), rabbit anti-phosphorylated (p-) AKT (ser473) polyclonal antibody (1:500, Cat# 11054, SAB), rabbit anti-GSK3β polyclonal antibody (1:600, Cat# 21002, SAB), rabbit anti-p-GSK3β (ser9) polyclonal antibody (1:600, Cat# 11002, SAB), and mouse anti-glyceraldehyde 3-phosphate dehydrogenase monoclonal antibody (1:1000, Cat# AF5009, Beyotime Biotechnology,). The next day, membranes were rinsed three times with Tris-buffered saline with Tween-20, and then incubated with goat anti-rabbit IgG secondary antibody (1:5000, Cat# L3012-2, SAB) or goat anti-mouse IgG secondary antibody (1:5000, Cat# L3032-2, SAB) for 1 hour. After detection and imaging of the phosphorylated protein, the membranes were stripped of the bound antibodies using Western Stripping buffer (Beyotime Biotechnology), then re-blocked for 2 hours at room temperature, followed by re-incubation with rabbit anti-AKT primary antibody (1:500, Cat# 40567, SAB), rabbit anti-GSK3β primary antibody (1:600, Cat# 21002, SAB) and the goat anti-rabbit IgG secondary antibody (1:5000, Cat# L3012-2, SAB) to detect the total protein. A chemiluminescence system (Bio-Rad, Berkeley, CA, USA) was used for protein visualization and ImageJ software was used for grayscale analysis. The protein expression levels were normalized with glyceraldehyde 3-phosphate dehydrogenase expression, and the phosphorylated protein expression levels were compared with their corresponding total protein level.

Statistical analysis

All data were statistically analyzed with SPSS 16.0 software (SPSS, Chicago, IL, USA). Data were expressed as the mean ± standard error of the mean (SEM). For comparisons between multiple groups, one-way analysis of variance was used when the variance was homogeneous; otherwise the Kruskal–Wallis test was used. Kaplan-Meier survival analysis was applied to assess survival rates. For mortality, Chi-square and Fisher exact tests were performed as appropriate. A statistically significant difference was considered as P-value < 0.05.

Results

Intranasal insulin reduces mortality and improves neurological function after ICH

We examined the effect of intranasal insulin on mortality rate and neurological damage after cerebral hemorrhage by survival analysis and NDS, respectively (n = 30 per group). The survival analysis showed that 1 IU intranasal insulin treatment significantly improved the survival rate compared with the normal saline treatment (P = 0.001; **Figure 1A**). In addition, the 1 IU intranasal insulin treatment group had significantly reduced mortality rates 24 hours (P = 0.002) and 72 hours (P = 0.002) after ICH, when compared with those in the saline treatment group. However, 0.5 and 2 IU insulin had no obvious effect in reducing the death rate (**Figure 1B** and **C**).

NDS showed that ICH mice had obvious neurological damage compared with the sham operation mice. Treatment with 1 IU intranasal insulin, but not 0.5 or 2 IU, significantly reduced the NDS at 24 (P = 0.009) and 72 hours (P = 0.011) after ICH compared with saline treatment, which indicated that 1 IU intranasal insulin reduced neurological impairment caused by ICH (**Figure 1D** and **E**).

Intranasal insulin reduces brain edema, BBB permeability, and hematoma volume after ICH

To further examine whether intranasal insulin could reduce brain injury after cerebral hemorrhage, brain water content (n = 6 per group), BBB permeability (n = 6 per group) and hematoma volume (n = 3 per group) were evaluated at 24 and 72 hours after the autologous blood injection surgery.

The extent of brain edema was assessed by brain water content of the ipsilateral brain tissue, contralateral brain tissue, and cerebellum. Compared with the sham group,

the ICH groups showed a significant increase in brain water content in the ipsilateral brain at 24 and 72 hours after surgery. Mice treated with 1 IU intranasal insulin showed a significant reduction in ipsilateral brain water content at 24 (P = 0.025) and 72 hours (P = 0.011) after ICH compared with mice treated with intranasal saline (**Figure 2A** and **B**). The water content of the contralateral brain tissue and cerebellum was similar between all groups.

BBB permeability was assessed by Evans blue staining. The permeability to Evans blue and hematoma volume were significantly increased in the ICH groups compared with the sham surgery group, which indicated that both the BBB and brain tissue were compromised. However, at 24 and 72 hours after ICH, the 1 IU intranasal insulin group had significantly reduced permeability to Evans blue (24 hours, P = 0.017; 72 hours, P = 0.034; **Figure 2C** and **D**) and reduced hematoma volume (24 hours, P = 0.021; 72 hours, P = 0.035; **Figure 2E–G**) compared with the normal saline group, indicating that intranasal insulin treatment alleviated the BBB disruption.

Intranasal insulin attenuates neuronal degeneration after ICH

On the basis of the above results, the sham, normal saline and 1 IU intranasal insulin groups (n = 3 per group) were chosen to assess neuronal degeneration in the perihematomal region by FJB staining. There were obvious degenerative neurons in the perihematomal brain tissues after ICH surgery. The number of FJB-positive cells in the perihematomal region in the intranasal insulin group was significantly lower than that in the normal saline group (P = 0.01; **Figure 3**). Therefore, intranasal insulin treatment attenuated neuronal degeneration after ICH.

Intranasal insulin activates the AKT/GSK3β signaling pathway

The AKT/GSK3β pathway is an important insulin signaling pathway, and is associated with BBB destruction, neuronal apoptosis, degeneration and necrosis (Li et al., 2018; He et al., 2019; Madugula et al., 2019). Therefore, we measured the expression of related proteins by western blotting to explore whether intranasal insulin exerts its effect via the AKT/GSK3β signaling pathway after ICH.

There were no significant differences in AKT and GSK3β expression between the groups. In contrast, p-AKT expression was increased in the intranasal insulin group compared with the normal saline group (P = 0.001; **Figure 4A** and **B**). Moreover, intranasal insulin-treated mice had significantly higher levels of p-GSK3β expression than saline-treated mice (P = 0.001; **Figure 4C** and **D**). These results suggested that intranasal insulin modulated the activation of the AKT/GSK3β signaling pathway.

Discussion

The purpose of our study was to explore whether intranasal insulin ameliorates neurological impairment after ICH and to identify the possible mechanisms underlying this effect. The autologous blood striatum injection model was used to simulate ICH in mice. A previous study reported that neurological damage was observed at 24 hours after autologous blood injection, and the injury was most severe at 72 hours (Wang et al., 2013). Thus, in this study, we used 24 and 72 hours as the time points to explore the effects of different doses of intranasal insulin on ICH in mice.

We determined whether intranasal insulin has a neuroprotective effect in ICH by assessing survival and NDS. We found that 1 IU of intranasal insulin significantly decreased the mortality and neurobehavioral deficits induced by ICH in mice. These findings supported our hypothesis that intranasal insulin improves the prognosis of ICH. Insulin resistance is closely associated with the occurrence of stroke and may be an independent risk factor for stroke (Kernan et al., 2002). As an alternative route of administration, intranasal insulin can elevate brain insulin concentration rapidly, efficiently, and safely, and also reduce insulin resistance (Costantino et al., 2007). Our results suggested that intranasal insulin may also exert a neuroprotective effect in cerebral hemorrhage, which manifested as reduced mortality, improved neurological function, and reduced pathological injury in experimental ICH mice.

In this study, we investigated the impact of intranasal insulin therapy on brain tissue damage caused by experimental cerebral hemorrhage. In the initial hours of ICH onset, the primary injury is caused by the mechanical compression and destruction of the perihematoma tissues by the hematoma, which causes secondary ischemia and hypoxia in adjacent tissues (Fang et al., 2019). Ischemia, hypoxia, and cell necrosis of numerous neurovascular units surrounding the hematoma can increase BBB permeability. Simultaneously, the lysis of massive amounts of spilled red blood cells and inflammation activation further aggravate the BBB destruction, which promotes the formation of brain edema (Wilkinson et al., 2018). Accordingly, hematoma volume, extent of cerebral edema, and BBB permeability can reflect the level of brain tissue damage after ICH in mice. We found that administering 1 IU of intranasal insulin markedly reduced the hematoma volume, extent of cerebral edema and BBB permeability caused by ICH in mice. This provides further evidence that intranasal insulin can reduce the degree of brain injury after ICH, which in turn alleviates damage to neural functions, reduces mortality, and improves prognosis.

We found that intranasal insulin had a neuroprotective effect in ICH in mice, and the 1 IU dose had the most pronounced effect, whereas the 2 IU dose had no significant beneficial effect. A potential reason for this result may be that intranasal insulin regulates cerebral blood flow in a dose-dependent manner, and excessive vasodilatation in the ICH focal area may exacerbate brain injury. Previous studies have shown that insulin, as a vasoactive hormone, can regulate cerebral blood flow, which can manifest as vasodilatation (Hughes and Craft, 2016) or vasoconstriction (Muniyappa and Yavuz, 2013). After our initial findings, we chose 1 IU intranasal insulin to further probe the mechanism of the neuroprotective effect. Intranasal insulin has been shown to improve cognitive impairment and attenuate neurological impairment in Alzheimer's disease and ischemic stroke via activation of the AKT/GSK3β signaling pathway (Lin et al., 2009; Li et al., 2019). AKT is activated by phosphorylation at Ser 437 after insulin binds to its receptor, and the activated AKT promotes phosphorylation of GSK3β at Ser9, which inactivates GSK3β (Manning and Toker, 2017). GSK3β has been associated with neuronal death, excessive GSK3β activation can induce neuronal degeneration (Madugula et al., 2019) and increase neuronal death in response to cell stress (Thornton et al., 2018). Our study also found that the expression of phosphorylated AKT (Ser473) and GSK3β (Ser9) in perihematoma tissues was significantly increased after intranasal insulin treatment, and the number of degenerative neurons was significantly decreased, suggesting that intranasal insulin decreased neuronal degeneration damage by activating the AKT/GSK3β insulin signaling pathway. Li et al. (2018) showed that inhibiting GSK3β activation increased the expression of claudin-1 and claudin-3, which are the main constituents of BBB tight junctions, thereby improving BBB integrity in experimental ICH animals. Our study showed consistent results in terms of improving BBB permeability. Therefore, we speculate that intranasal insulin also reduced BBB damage via the AKT/GSK3β signaling pathway as part of its neuroprotective effect in mice after ICH.

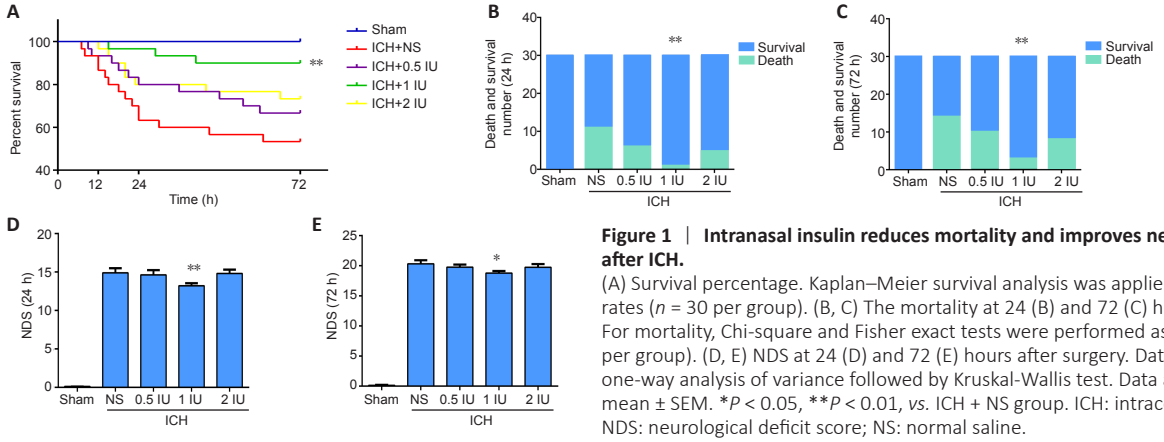

Figure 1 | Intranasal insulin reduces mortality and improves neurological function after ICH.
(A) Survival percentage. Kaplan–Meier survival analysis was applied to assess survival rates (n = 30 per group). (B, C) The mortality at 24 (B) and 72 (C) hours after operation. For mortality, Chi-square and Fisher exact tests were performed as appropriate (n = 30 per group). (D, E) NDS at 24 (D) and 72 (E) hours after surgery. Data were analyzed by one-way analysis of variance followed by Kruskal-Wallis test. Data are expressed as the mean ± SEM. *P < 0.05, **P < 0.01, *vs.* ICH + NS group. ICH: intracerebral hemorrhage; NDS: neurological deficit score; NS: normal saline.

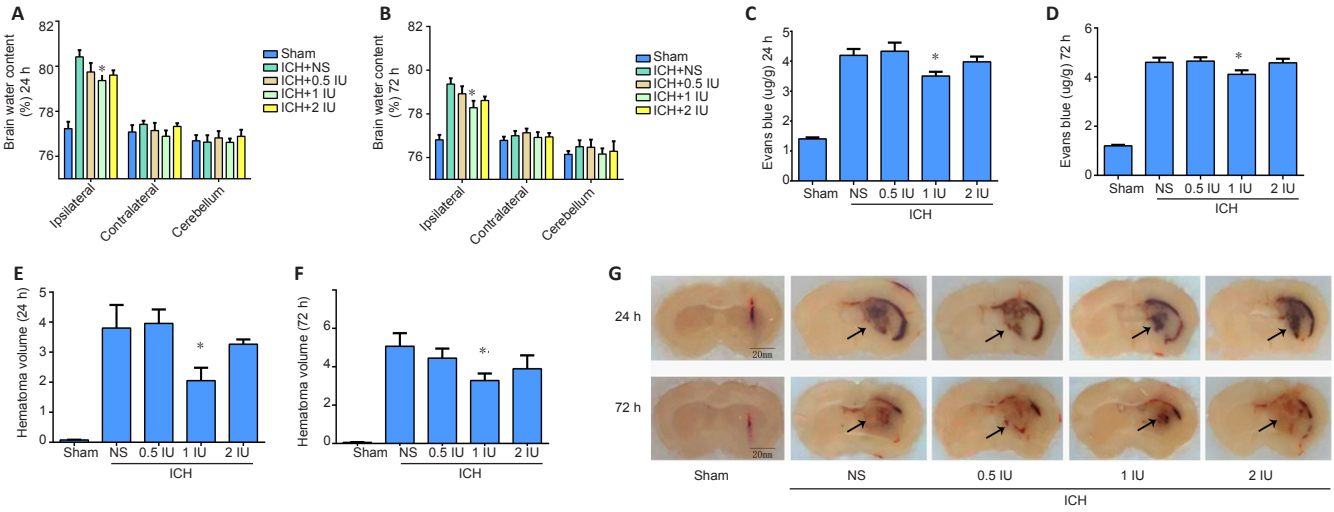

Figure 2 | Intranasal insulin reduces brain edema, blood-brain barrier permeability and hematoma volume after ICH.
(A, B) Brain water content of the ipsilateral brain tissue, contralateral brain tissue, and cerebellum at 24 (A) and 72 (B) hours after surgery in mice. (C, D) The permeability to Evans blue at 24 (C) and 72 (D) hours after surgery, which is an indicator of blood-brain barrier permeability. (E, F) Hematoma volume at 24 (E) and 72 (F) hours after surgery. Data are expressed as the mean ± SEM (A–D: n = 6 per group; E–F: n = 3 per group). *P < 0.05, *vs.* ICH + NS group (one-way analysis of variance followed by Kruskal-Wallis test). (G) The extent of the hematoma induced by ICH in coronal sections. Decreased hematoma volume was observed in ICH mice treated with 1 IU intranasal insulin. The arrows indicate the hematoma. Scale bars: 20 mm. ICH: Intracerebral hemorrhage; NS: normal saline.

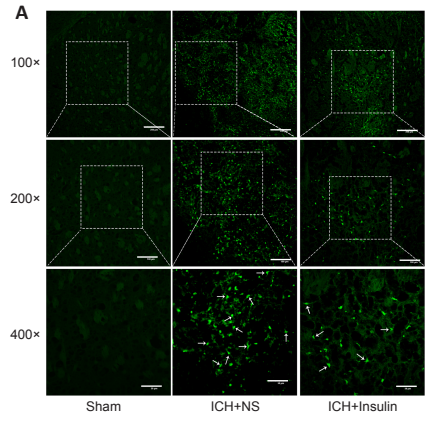

Figure 3 | Intranasal insulin attenuates neuronal degeneration after ICH.
FJB staining showed that ICH resulted in neuronal degeneration damage and intranasal insulin treatment significantly attenuated neuronal degeneration. (A) FJB-positive neurons (green; stained by Alexa Fluor-488) in sham mice and ICH mice treated with intranasal NS or 1 IU intranasal insulin were observed with fluorescence microscopy to measure neuronal degeneration. The white arrows indicate the FJB-positive neurons. Scale bars: 200 μm for 100×, 100 μm for 200×, 50 μm for 400×. (B) Quantitative statistics of FJB-positive cell number. Data are expressed as the mean ± SEM (n = 3 per group). **P < 0.01, *vs.* ICH + NS group (one-way analysis of variance followed by Kruskal-Wallis test). FJB: Fluoro-Jade B; ICH: intracerebral hemorrhage; NS: normal saline.

Our study has some limitations that may require further studies to address. Our findings suggested that intranasal insulin played a neuroprotective role through the AKT/GSK3β signaling pathway. However, AKT is a multifunctional enzyme and we did not use specific pathway inhibitors in our study. Therefore, we cannot exclude the possible regulation by AKT on other downstream signaling molecules, such as caspase-3, NF-κB, or nitric oxide synthase, which are associated with apoptosis, inflammation, and vascular regulation (Tang et al., 2016; Icli et al., 2019; Luo et al., 2019). These potential mechanisms warrant further investigation. Additionally, intranasal insulin was only administered until 72 hours after the operation in our study. Despite the reduction of brain injury and improvement of neural function by intranasal insulin that were observed during that period, it remains uncertain whether continued intervention would lead to stronger effects. Additionally, our study found that the neurological function of the ICH mice did not improve significantly after intervention with 2 IU intranasal insulin. We speculated that the reason was related to the regulation of cerebral blood flow by different doses of insulin. However, the effect of 2 IU intranasal insulin on cerebral vessels was not

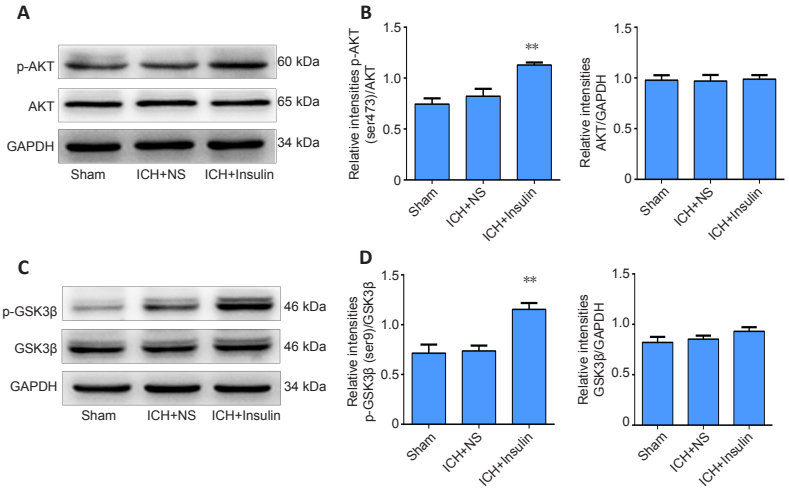

Figure 4 | Intranasal insulin activates the AKT/GSK3β signaling pathway.
(A) Western blot showing protein expression of p-AKT (ser473) and AKT proteins in sham mice and ICH mice treated with intranasal NS or 1 IU intranasal insulin. (B) The phosphorylation and protein expression of AKT. (C) Western blot showing protein expression of p-GSK3β (ser9) and GSK3β. (D) The phosphorylation and protein expression of GSK3β. Data are expressed as the mean ± SEM (n = 6 per group). $^{**}P < 0.01$, *vs.* ICH + NS group (one-way analysis of variance followed by Kruskal-Wallis test). GAPDH: Glyceraldehyde 3-phosphate dehydrogenase; ICH: intracerebral hemorrhage; NS: normal saline.

directly confirmed in this study.

In conclusion, our findings indicate that intranasal insulin mitigated the hematoma volume and brain edema, thus ameliorating neurological impairment, elevating survival rate, and improving prognosis in ICH model mice. These outcomes occurred in parallel with an improvement of BBB permeability, reduction of neuronal degeneration damage, and elevation of p-AKT and p-GSK3β expression. We conclude that intranasal insulin ameliorated neurological impairment after ICH, and that the potential mechanism of the effect was AKT/GSK3β signaling pathway activation. Thus, our findings support further study of intranasal insulin as a treatment for ICH and AKT/GSK3β pathway should be investigated for potential drug targets for ICH.

Author contributions: *Study conception and design: GHJ, JMY, XMW, YZ. Experiment implementation and data collection: YZ ,YH, JY, RT, XZ, WWH. Statistical analysis: YZ, YH ,CYH. Manuscript drafting: YZ, YH. Manuscript revising: GHJ, JMY. All authors approved the final version of the manuscript.*
Conflicts of interest: *The authors declare no conflict of interest.*
Financial support: *This work was supported by the National Natural Science Foundation of China, No. 81971220; and a grant from the Science and Technology Department of Sichuan Province of China, No. 2018JY0236 (both to GHJ). The funding sources had no role in study conception and design, data analysis or interpretation, paper writing or deciding to submit this paper for publication.*
Institutional review board statement: *The study was approved by the Ethics Committee of the North Sichuan Medical College (Nanchong, China; approval No. NSMC(A)2019(01)) on January 7, 2019.*

Data sharing statement: *Datasets analyzed during the current study are available from the corresponding author on reasonable request.*
Plagiarism check: *Checked twice by iThenticate.*
Peer review: *Externally peer reviewed.*

Additional file:
Additional Table 1: *Neurological deficit scoring system.*

References

An SJ, Kim TJ, Yoon BW (2017) Epidemiology, risk factors, and clinical features of intracerebral hemorrhage: an update. J Stroke 19:3-10.

Arnold SE, Arvanitakis Z, Macauley-Rambach SL, Koenig AM, Wang HY, Ahima RS, Craft S, Gandy S, Buettner C, Stoeckel LE, Holtzman DM, Nathan DM (2018) Brain insulin resistance in type 2 diabetes and Alzheimer disease: concepts and conundrums. Nat Rev Neurol 14:168-181.

Auriat A, Plahta WC, McGie SC, Yan R, Colbourne F (2005) 17beta-Estradiol pretreatment reduces bleeding and brain injury after intracerebral hemorrhagic stroke in male rats. J Cereb Blood Flow Metab 25:247-256.

Begg DP (2015) Insulin transport into the brain and cerebrospinal fluid. Vitam Horm 98:229-248.

Chang CF, Chen SF, Lee TS, Lee HF, Chen SF, Shyue SK (2011) Caveolin-1 deletion reduces early brain injury after experimental intracerebral hemorrhage. Am J Pathol 178:1749-1761.

Clark W, Gunion-Rinker L, Lessov N, Hazel K (1998) Citicoline treatment for experimental intracerebral hemorrhage in mice. Stroke 29:2136-2140.

Costantino HR, Illum L, Brandt G, Johnson PH, Quay SC (2007) Intranasal delivery: physicochemical and therapeutic aspects. Int J Pharm 337:1-24.

Fang Y, Tian Y, Huang Q, Wan Y, Xu L, Wang W, Pan D, Zhu S, Xie M (2019) Deficiency of TREK-1 potassium channel exacerbates blood-brain barrier damage and neuroinflammation after intracerebral hemorrhage in mice. J Neuroinflammation 16:96.

Gabbouj S, Natunen T, Koivisto H, Jokivarsi K, Takalo M, Marttinen M, Wittrahm R, Kemppainen S, Naderi R, Posado-Fernández A, Ryhänen S, Mäkinen P, Paldanius KMA, Doria G, Poutiainen P, Flores O, Haapasalo A, Tanila H, Hiltunen M (2019) Intranasal insulin activates Akt2 signaling pathway in the hippocampus of wild-type but not in APP/PS1 Alzheimer model mice. Neurobiol Aging 75:98-108.

GBD 2016 Stroke Collaborators (2019) Global, regional, and national burden of stroke, 1990-2016: a systematic analysis for the Global Burden of Disease Study 2016. Lancet Neurol 18:439-458.

Ghasemi R, Haeri A, Dargahi L, Mohamed Z, Ahmadiani A (2013) Insulin in the brain: sources, localization and functions. Mol Neurobiol 47:145-171.

He H, Li X, He Y (2019) Hyperbaric oxygen therapy attenuates neuronal apoptosis induced by traumatic brain injury via Akt/GSK3β/β-catenin pathway. Neuropsychiatr Dis Treat 15:369-374.

Huang SS, Lu YJ, Huang JP, Wu YT, Day YJ, Hung LM (2014) The essential role of endothelial nitric oxide synthase activation in insulin-mediated neuroprotection against ischemic stroke in diabetes. J Vasc Surg 59:483-491.

Hughes TM, Craft S (2016) The role of insulin in the vascular contributions to age-related dementia. Biochim Biophys Acta 1862:983-991.

Icli B, Wu W, Ozdemir D, Li H, Cheng HS, Haemmig S, Liu X, Giatsidis G, Avci SN, Lee N, Guimaraes RB, Manica A, Marchini JF, Rynning SE, Risnes I, Hollan I, Croce K, Yang X, Orgill DP, Feinberg MW (2019) MicroRNA-615-5p regulates angiogenesis and tissue repair by targeting AKT/eNOS (protein kinase B/endothelial nitric oxide synthase) signaling in endothelial cells. Arterioscler Thromb Vasc Biol 39:1458-1474.

Keep RF, Hua Y, Xi G (2012) Intracerebral haemorrhage: mechanisms of injury and therapeutic targets. Lancet Neurol 11:720-731.

Keep RF, Andjelkovic AV, Xiang J, Stamatovic SM, Antonetti DA, Hua Y, Xi G (2018) Brain endothelial cell junctions after cerebral hemorrhage: Changes, mechanisms and therapeutic targets. J Cereb Blood Flow Metab 38:1255-1275.

Kernan WN, Inzucchi SE, Viscoli CM, Brass LM, Bravata DM, Horwitz RI (2002) Insulin resistance and risk for stroke. Neurology 59:809-815.

Krishnamurthi RV, Feigin VL, Forouzanfar MH, Mensah GA, Connor M, Bennett DA, Moran AE, Sacco RL, Anderson LM, Truelsen T, O'Donnell M, Venketasubramanian N, Barker-Collo S, Lawes CM, Wang W, Shinohara Y, Witt E, Ezzati M, Naghavi M, Murray C (2013) Global and regional burden of first-ever ischaemic and haemorrhagic stroke during 1990-2010: findings from the Global Burden of Disease Study 2010. Lancet Glob Health 1:e259-281.

Li W, Li R, Zhao S, Jiang C, Liu Z, Tang X (2018) Lithium posttreatment alleviates blood-brain barrier injury after intracerebral hemorrhage in rats. Neuroscience 383:129-137.

Li X, Run X, Wei Z, Zeng K, Liang Z, Huang F, Ke D, Wang Q, Wang JZ, Liu R, Zhang B, Wang X (2019) Intranasal insulin prevents anesthesia-induced cognitive impairments in aged mice. Curr Alzheimer Res 16:8-18.

Lin S, Fan LW, Rhodes PG, Cai Z (2009) Intranasal administration of IGF-1 attenuates hypoxic-ischemic brain injury in neonatal rats. Exp Neurol 217:361-370.

Lioutas VA, Novak V (2016) Intranasal insulin neuroprotection in ischemic stroke. Neural Regen Res 11:400-401.

Liu AH, Wu YT, Wang YP (2017) MicroRNA-129-5p inhibits the development of autoimmune encephalomyelitis-related epilepsy by targeting HMGB1 through the TLR4/NF-kB signaling pathway. Brain Res Bull 132:139-149.

Luo R, Chen X, Ma H, Yao C, Liu M, Tao J, Li X (2019) Myocardial caspase-3 and NF-κB activation promotes calpain-induced septic apoptosis: The role of Akt/eNOS/NO pathway. Life Sci 222:195-202.

Lv H, Tang L, Guo C, Jiang Y, Gao C, Wang Y, Jian C (2020) Intranasal insulin administration may be highly effective in improving cognitive function in mice with cognitive dysfunction by reversing brain insulin resistance. Cogn Neurodyn 14:323-338.

Madugula K, Mulherkar R, Khan ZK, Chigbu DI, Patel D, Harhaj EW, Jain P (2019) MEF-2 isoforms' (A-D) roles in development and tumorigenesis. Oncotarget 10:2755-2787.

Manning BD, Toker A (2017) AKT/PKB signaling: navigating the network. Cell 169:381-405.

Meng Z, Zhao T, Zhou K, Zhong Q, Wang Y, Xiong X, Wang F, Yang Y, Zhu W, Liu J, Liao M, Wu L, Duan C, Li J, Gong Q, Liu L, Xiong A, Yang M, Wang J, Yang Q (2017) A20 ameliorates intracerebral hemorrhage-induced inflammatory injury by regulating TRAF6 polyubiquitination. J Immunol 198:820-831.

Muniyappa R, Yavuz S (2013) Metabolic actions of angiotensin II and insulin: a microvascular endothelial balancing act. Mol Cell Endocrinol 378:59-69.

Ramesh SS, Christopher R, Indira Devi B, Bhat DI (2019) The vascular protective role of oestradiol: a focus on postmenopausal oestradiol deficiency and aneurysmal subarachnoid haemorrhage. Biol Rev Camb Philos Soc 94:1897-1917.

Rhea EM, Banks WA (2019) Role of the blood-brain barrier in central nervous system insulin resistance. Front Neurosci 13:521.

Santiago JCP, Hallschmid M (2019) Outcomes and clinical implications of intranasal insulin administration to the central nervous system. Exp Neurol 317:180-190.

Shao Z, Tu S, Shao A (2019) Pathophysiological mechanisms and potential therapeutic targets in intracerebral hemorrhage. Front Pharmacol 10:1079.

Song EC, Chu K, Jeong SW, Jung KH, Kim SH, Kim M, Yoon BW (2003) Hyperglycemia exacerbates brain edema and perihematomal cell death after intracerebral hemorrhage. Stroke 34:2215-2220.

Tang B, Tang F, Wang Z, Qi G, Liang X, Li B, Yuan S, Liu J, Yu S, He S (2016) Upregulation of Akt/NF-κB-regulated inflammation and Akt/Bad-related apoptosis signaling pathway involved in hepatic carcinoma process: suppression by carnosic acid nanoparticle. Int J Nanomedicine 11:6401-6420.

Thornton TM, Hare B, Colié S, Pendlebury WW, Nebreda AR, Falls W, Jaworski DM, Rincon M (2018) Failure to inactivate nuclear GSK3β by Ser(389)-phosphorylation leads to focal neuronal death and prolonged fear response. Neuropsychopharmacology 43:393-405.

Wang X, Kang K, Wang S, Yao J, Zhang X (2016) Focal cerebral ischemic tolerance and change in blood-brain barrier permeability after repetitive pure oxygen exposure preconditioning in a rodent model. J Neurosurg 125:943-952.

Wang YC, Wang PF, Fang H, Chen J, Xiong XY, Yang QW (2013) Toll-like receptor 4 antagonist attenuates intracerebral hemorrhage-induced brain injury. Stroke 44:2545-2552.

Wieberdink RG, Koudstaal PJ, Hofman A, Witteman JC, Breteler MM, Ikram MA (2012) Insulin resistance and the risk of stroke and stroke subtypes in the nondiabetic elderly. Am J Epidemiol 176:699-707.

Wilkinson DA, Pandey AS, Thompson BG, Keep RF, Hua Y, Xi G (2018) Injury mechanisms in acute intracerebral hemorrhage. Neuropharmacology 134:240-248.

Xiao H, Deng M, Yang B, Tang J, Hu Z (2017) Role of glycogen synthase kinase 3 in ischemia-induced blood-brain barrier disruption in aged female rats. J Neurochem 142:194-203.

Yang Y, Ma D, Wang Y, Jiang T, Hu S, Zhang M, Yu X, Gong CX (2013) Intranasal insulin ameliorates tau hyperphosphorylation in a rat model of type 2 diabetes. J Alzheimers Dis 33:329-338.

Zeng Y, Zhang L, Hu Z (2016) Cerebral insulin, insulin signaling pathway, and brain angiogenesis. Neurol Sci 37:9-16.

Zheng H, Chen C, Zhang J, Hu Z (2016) Mechanism and therapy of brain edema after intracerebral hemorrhage. Cerebrovasc Dis 42:155-169.

Zhou K, Zhong Q, Wang YC, Xiong XY, Meng ZY, Zhao T, Zhu WY, Liao MF, Wu LR, Yang YR, Liu J, Duan CM, Li J, Gong QW, Liu L, Yang MH, Xiong A, Wang J, Yang QW (2017) Regulatory T cells ameliorate intracerebral hemorrhage-induced inflammatory injury by modulating microglia/macrophage polarization through the IL-10/GSK3β/PTEN axis. J Cereb Blood Flow Metab 37:967-979.

Zhu W, Gao Y, Chang CF, Wan JR, Zhu SS, Wang J (2014) Mouse models of intracerebral hemorrhage in ventricle, cortex, and hippocampus by injections of autologous blood or collagenase. PLoS One 9:e97423.

C-Editor: Zhao M; S-Editors: Yu J, Li CH; L-Editors: McCollum L, Yu J, Song LP; T-Editor: Jia Y

Additional Table 1 Neurological deficit scoring system

	0	1	2	3	4
(1) Body symmetry (open bench top)	Normal	Slight asymmetry	Moderate asymmetry	Prominent symmetry	Extreme asymmetry
(2) Gait (open bench top)	Normal	Stiff, Inflexible	Limping	Trembling, drifting, falling	Does not walk
(3) Climbing gripping surface, 45° angle)	Normal	Climbs with strain, limb weakness resent	Holds onto slope, does not slip or climb	Slides down slope, unsuccessful effort to prevent fall	Slides immediately, no effort to prevent fall
(4) Circling behavior (open bench top)	Not present	Predominantly one-sided turns	Circles to one side (not constantly)	Circles constantly to one side	Pivoting, swaying, or no movement
(5) Front limb symmetry (mouse suspended by its tail)	Normal	Light asymmetry	Marked asymmetry	Prominent symmetry	Slight asymmetry, no body/limb movement
(6) Compulsory circling (front limbs on bench, rear suspended by tail)	Not present	Tendency to turn to one side	Circles to one side	Pivots to one side sluggishly	Does not advance
(7) Whisker response (light touch from behind)	Symmetrical response	Light asymmetry	Prominent asymmetry	Absent response ipsilaterally, diminished contralaterally	Absent proprioceptive response bilaterally

The neurological deficit score is the total score of seven categories, which are each given a score from 0–4.